arXiv:2505.06557v1 [cs.CV] 10 May 2025

Weakly Supervised Temporal Sentence Grounding via Positive Sample Mining

Lu Dong, Haiyu Zhang, Hongjie Zhang, Yifei Huang, Zhen-Hua Ling, *Senior Member, IEEE*, Yu Qiao, *Senior Member, IEEE*, Limin Wang, *Member, IEEE*, Yali Wang

***Abstract*—The task of weakly supervised temporal sentence grounding (WSTSG) aims to detect temporal intervals corresponding to a language description from untrimmed videos with only video-level video-language correspondence. For an anchor sample, most existing approaches generate negative samples either from other videos or within the same video for contrastive learning. However, some training samples are highly similar to the anchor sample, directly regarding them as negative samples leads to difficulties for optimization and ignores the correlations between these similar samples and the anchor sample. To address this, we propose Positive Sample Mining (PSM), a novel framework that mines positive samples from the training set to provide more discriminative supervision. Specifically, for a given anchor sample, we partition the remaining training set into semantically similar and dissimilar subsets based on the similarity of their text queries. To effectively leverage these correlations, we introduce a PSM-guided contrastive loss to ensure that the anchor proposal is closer to similar samples and further from dissimilar ones. Additionally, we design a PSM-guided rank loss to ensure that similar samples are closer to the anchor proposal than to the negative intra-video proposal, aiming to distinguish the anchor proposal and the negative intra-video proposal. Experiments on the WSTSG and grounded VideoQA tasks demonstrate the effectiveness and superiority of our method.**

***Index Terms*—Temporal sentence grounding, weakly supervised learning, contrastive learning, rank loss.**

I. Introduction

TEMPORAL sentence grounding is a fundamental task for video understanding, where the goal is to locate the start and end timestamps of one segment in the video that semantically corresponds to the given sentence query. This task has the potential for a wide range of applications such as video summarization [1], [2], [3], video retrieval [4], [5], [6] and human-computer interaction systems [7], [8], [9]. For temporal sentence grounding, the supervised approaches [10], [11], [12] have achieved impressive results but heavily rely on manual annotations of temporal locations for each query-video pair. The annotation process is both time-consuming and label-intensive, limiting the scalability of these methods.

To address this limitation, weakly supervised temporal sentence grounding (WSTSG) approaches [10], [13], [14], [15], [16], [17] have been proposed, requiring only query-video pairs without temporal annotations for training. This reduces the dependency on manual labeling, enabling the use of large-scale data that is readily available online, as query-video pairs can be easily obtained from the Internet. Due to the absence of temporal annotations, most previous studies mine negative samples from the training set for contrastive learning, aiming to provide supervision signals for generating proposals. These weakly supervised methods for temporal sentence grounding are broadly categorized into multiple instance learning (MIL)-based

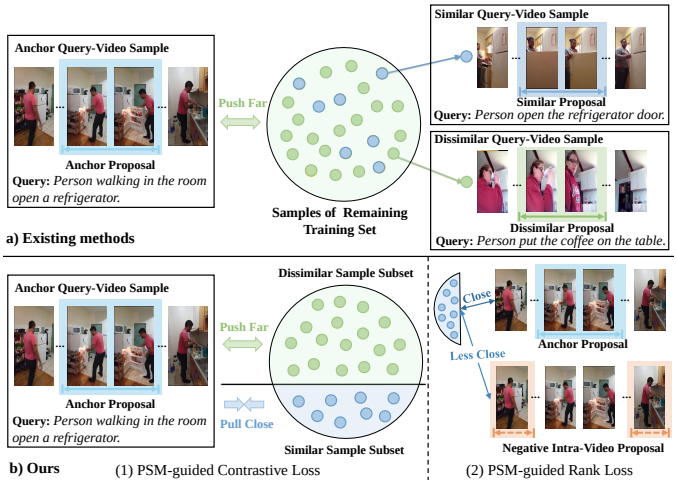

Fig. 1: a) Existing methods regard all samples in the remaining training set as negative and push them further from the anchor proposal, which ignores the diversity of the training set. b) Our method mines similar training samples for each anchor sample to leverage more discriminative supervision from other video samples. Two schemes are proposed. 1) A PSM-guided contrastive loss is proposed to distinguish between similar and dissimilar sample pairs. 2) A PSM-guided rank loss is proposed to improve the distinction between the anchor proposal and the negative intra-video proposal.

Lu Dong is with University of Science and Technology of China, Hefei 230027, China, and also with Shanghai Artificial Intelligence Laboratory, Shanghai 202150, China. (Email: dl1111@mail.ustc.edu.cn)

Haiyu Zhang is with Beihang University, Beijing 100191, China, and also with Shanghai Artificial Intelligence Laboratory, Shanghai 202150, China. (Email: zhyzhy@buaa.edu.cn)

Hongjie Zhang, Yifei Huang, and Yu Qiao are with Shanghai Artificial Intelligence Laboratory, Shanghai 202150, China. (Email: nju.zhanghongjie@gmail.com, hyf015@gmail.com, and yu.qiao@siat.ac.cn)

Zhen-Hua Ling is with University of Science and Technology of China, Hefei 230027, China (Email: zhling@ustc.edu.cn)

Limin Wang is with State Key Laboratory for Novel Software Technology, Nanjing University, Nanjing 210023, China, and also with Shanghai Artificial Intelligence Laboratory, Shanghai 202150, China. (Email: lmwang@nju.edu.cn)

Yali Wang is with Shenzhen Key Laboratory of Computer Vision and Pattern Recognition, Shenzhen Institute of Advanced Technology, Chinese Academy of Sciences, Shenzhen 518055, China, and also with Shanghai Artificial Intelligence Laboratory, Shanghai 202150, China. (Email: yl.wang@siat.ac.cn). *Yali Wang is the corresponding author.*

Copyright © 2025 IEEE. Personal use of this material is permitted. However, permission to use this material for any other purposes must be obtained from the IEEE by sending an email to pubs-permissions@ieee.org.

and reconstruction-based approaches. Specifically, MIL-based approaches [10], [18], [19], [20] generate negative samples from mismatched query-video pairs (*e.g.*, a sentence query paired with a mismatched video in the training set). The model is trained to distinguish between matched (positive) and mismatched (negative) samples. On the other hand, reconstruction-based researches [21], [22], [23], [16], [17] generate negative proposals from segments within the same video, enhancing the model's ability to handle more confusing video segments.

Given an anchor query-video sample, all previous methods mine negative samples from the training set for contrastive training. However, they treat all samples of remaining training set equally, ignoring the inherent diversity among them. As shown in Fig. 1, for an anchor sample with the query "Person walking in the room open a refrigerator", there exists a very similar training sample with the query "Person open the refrigerator door". As they have the same object "refrigerator" and action "open", their corresponding proposal segments are also semantically similar. If these similar samples are treated as negative samples, the model is forced to push away samples that are semantically alike. This complicates optimization process and leads to suboptimal results. Therefore, for each anchor sample, the remaining training set should be partitioned into two subsets: a *similar* subset and a *dissimilar* subset, based on the similarity of each sample to the anchor sample. Different operations can then be applied to each subset to better leverage their unique characteristics.

Building on this insight, we propose Positive Sample Mining (PSM), a novel WSTSG framework that mines positive samples for each anchor sample, which aims to leverage more discriminative supervision from other video samples. Specifically, for an anchor sample, we first divide other samples in the remaining training set based on the semantic similarity of their text queries. This will result in a similar sample subset and a dissimilar sample subset. To discriminate these similar and dissimilar sample pairs, we propose a PSM-guided contrastive loss to ensure that the anchor proposal is closer to the similar subset and further from the dissimilar subset, thereby enhancing the model's ability to capture sophisticated semantic correlations in the sample space. Furthermore, we propose a PSM-guided rank loss to leverage the intra-video information, which guarantees that similar samples are closer to the anchor proposal than to the negative intra-video proposal. It can effectively enhance the distinction between the anchor proposal and the negative intra-video proposal.

In summary, our contributions are threefold:

- We propose a Positive Sample Mining (PSM) for the WSTSG task. To the best of our knowledge, this is *the first attempt* to mine positive samples within the training set for this task.
- We propose a PSM-guided contrastive loss to discriminate between similar and dissimilar samples. Furthermore, we design a PSM-guided rank loss to enhance the distinction between the anchor proposal and the negative intra-video proposal.
- We validate the effectiveness of our approach through comprehensive evaluations on two tasks: WSTSG and grounded VideoQA. Our approach achieves superior performance compared to existing methods.

II. Related Works

A. Fully Supervised Temporal Sentence Grounding

Many previous works [10], [24], [13], [25], [26], [27], [28], [29], [30], [31], [32], [33] focus on fully supervised temporal sentence grounding, where each query-video pair is annotated with precise start and end timestamps. TALL [10] first produces proposals of various lengths through sliding windows, then uses query-proposal fusion for moment regression. 2D-TAN [14] uses a two-dimensional map to model the temporal relation between proposal candidates, enabling an exhaustive enumeration of proposals with diverse durations. CRNet [31] formulates temporal sentence grounding as a video reading comprehension task, enabling the model to capture comprehensive relational information from multiple perspectives. P-Debias [33] investigates both visual and combinatorial biases within the training dataset to enhance the robustness of the training process. However, these methods require manual annotations of temporal locations for each query-video pair. These manual annotations are usually label-consuming and subjective (inconsistency among multiple annotators) [34], which ultimately harms the scalability of these approaches for real-world applications.

B. Weakly Supervised Temporal Sentence Grounding

To reduce annotation effects, the weakly supervised paradigm has gained increasing attention across various video tasks, such as temporal action localization [35], [36], [37], [38], [39], video instance segmentation [40], [41] and video anomaly detection [42], [43], [44]. Regarding temporal sentence grounding (TSG), the weakly supervised TSG methods use only video-level query-video correspondence during training, without requiring start and end timestamps. In the absence of explicit timestamp annotations, most existing approaches adopt the anchor text query and the anchor proposal as positive pairs and mine negative samples for contrastive learning. One group of methods adopts the multi-instance learning (MIL) approach [45], [18], [19], [46], [20]. These methods construct negative samples from mismatched query-video pairs (*e.g.*, an anchor video paired with a mismatched query in the training set). The model learns the video-level video-language correspondence by maximizing the matching scores of the positive pairs while penalizing those of the negative pairs. Reconstruction-based methods [21], [22], [23], [16], [47], [17] measure the query-proposal alignment by the reconstruction of the query, which provides more fine-grained information. Additionally, these methods mine easy and hard negative intra-video proposals to facilitate contrastive learning.

Both MIL-based and reconstruction-based methods treat all remaining samples in the training set as negative samples equally. However, they ignore the inherent diversity in the training set, where some samples are highly similar to the anchor sample. Therefore, the model sometimes would be forced to push away two samples that are highly similar, leading to difficulties for optimization. Moreover, these methods ignore

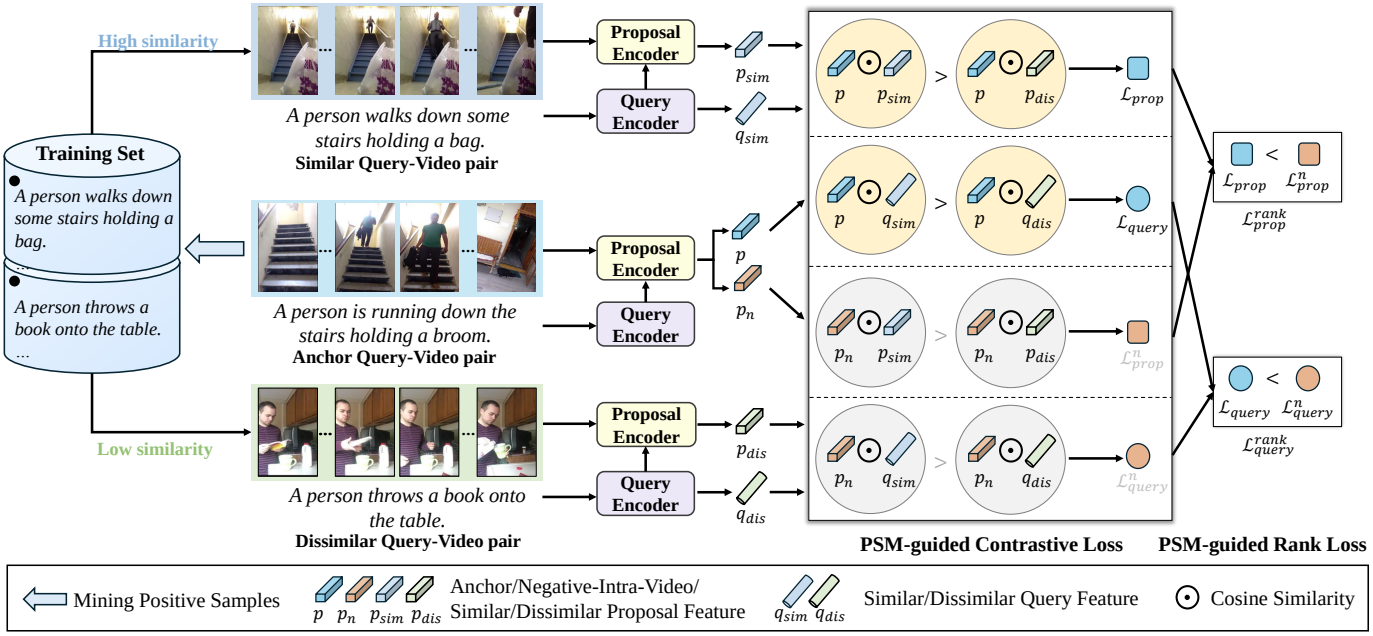

Fig. 2: Overview of our proposed method. First, we mine positive samples from the remaining training set to capture sophisticated semantic correlations in the sample space. Next, the proposal and query encoders are adopted to extract the global representations of proposals and queries. For similar and dissimilar query-video pairs, we utilize the positive proposal feature from the proposal encoder to compute the PSM-guided contrastive loss. Finally, PSM-guided contrastive loss is adopted to distinguish between similar and dissimilar queries/proposals for the anchor proposal. Furthermore, a PSM-guided rank loss improves the distinction between the anchor proposal and the negative intra-video proposal, based on the distance to similar samples (*i.e.*, the PSM guided contrastive loss).

the correlations between similar samples and the anchor sample. In contrast, our approach identifies the similar and dissimilar samples in the training set and ensures the anchor proposal is closer to the similar subset and further from the dissimilar subset, which alleviates the difficulty of capturing correlations between query-video samples and leverages more discriminative supervision from other video samples.

C. Negative Sample Mining

Negative sample mining [48], [49], [50], [51], [52], [53], [54] has been widely studied in metrics learning and has massive applications for supervised and weakly supervised TSG. Most of these methods observe that it is helpful to use negative samples that are difficult for the model to discriminate. [49] theoretically proves hard negative objectives can capture desirable generalization properties for contrastive learning. In supervised TSG, negative sample mining focuses on debiasing the shortcut of memorizing spurious correlations that link given queries to specific scenes. SQuiDNet [51] performs selective debiasing via disentangling good and bad retrieval bias based on the query meaning. CTDL [52] mitigates the bias of TSG training via contrasting factual retrievals with counterfactually biased retrievals. Multi-NA [53] proposes multiple negative augmentations to diversify the data distribution, which eases the problem of fitting the temporal distribution bias. BSSARD [54] introduces adversarial training on synthesized bias-conflicting samples to mitigate uneven temporal distributions of target moments. For weakly supervised TSG, current methodologies mine hard intra-video negative proposals for robust training. PPS [17] generates diverse negative proposals through multiple Gaussian masks. DSCE [55] gradually increases the difficulty of the negative proposal with a dual-signed cross-entropy loss. However, most of the existing methods treat the samples of the remaining training set equally, which ignores the inherent diversity among them. In contrast, our PSM partitions the remaining training set into similar and dissimilar subsets for each anchor sample and discriminates these similar and dissimilar samples, enhancing the model's ability to capture sophisticated semantic correlations in the sample space and providing more discriminative supervision for weakly supervised TSG.

D. Positive Inter-Sample Mining

Positive inter-sample mining approaches extract positive signals from other samples in the training set. The goal is to explore latent correlations and interactions between multiple data points. Positive inter-sample mining has various applications in computer vision, including image retrieval [56], [57], [58], domain adaptation [59], [60] and video object detection [61], [62]. CSD [56] mines similar images to establish a contextual similarity constraint on the anchor image, which effectively guides the learning process of lightweight query models. HVR-Net [61] identifies similar samples with distinct object labels, utilizing them as hard negative samples to improve the effectiveness of contrastive learning. To the best of our knowledge, we are the first to mine positive inter-video samples

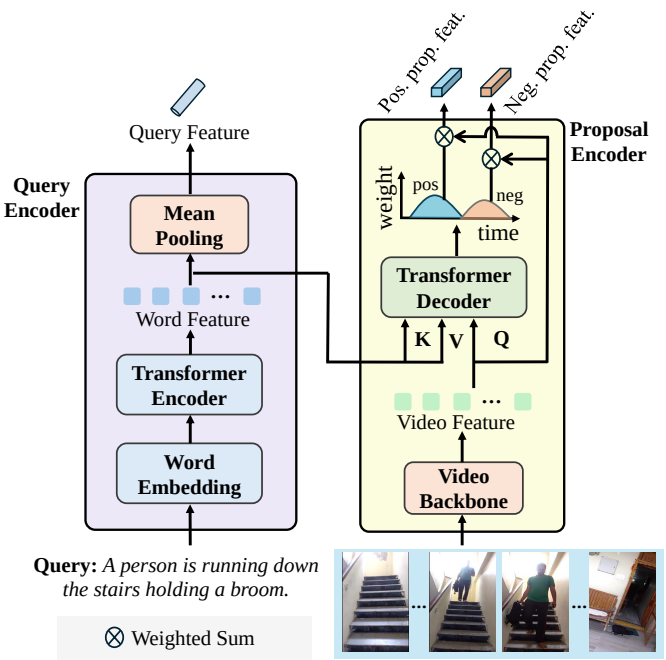

Fig. 3: The architecture of query and proposal encoder. The main network is adopted from CPL [16]. We add mean-pooling to extract the global query feature and employ weighted sum to extract global positive and negative proposal features.

for the weakly supervised temporal sentence grounding and demonstrate the effectiveness of our method.

III. Method

We first present the problem formulation of weakly supervised temporal sentence grounding. Given a video $\mathcal{V}$ and a query sentence $\mathcal{Q}$ that describes a sub-event within this video, the objective is to ground the sentence to a specific temporal segment within the video by predicting the start and end timestamps. During training, the ground truth of the timestamps is not available.

The overall architecture of our PSM is illustrated in Fig. 2. PSM consists of a proposal encoder, a query encoder, mining positive samples, and two PSM-guided losses. The query and proposal encoders extract the features of the query and the proposal using the transformer-based backbones [16], [17]. We then pool the query and proposal features to extract their global representations. In addition, we mine similar and dissimilar query-video sample pairs from the remaining training set to capture sophisticated semantic correlations in the sample space. To distinguish between similar and dissimilar sample pairs, we propose a PSM-guided contrastive loss to bring the anchor proposal closer to similar samples and further from dissimilar samples. Furthermore, we propose a PSM-guided rank loss to improve the distinction between the anchor proposal and the negative intra-video proposal. The PSM-guided rank loss ensures that the similar sample is closer to the anchor proposal than to the negative intra-video proposal.

A. Query and Proposal Encoders

The architectures of query and proposal encoders are illustrated in Fig. 3. Given a video and sentence query, we extract the global proposal and query representations using transformer-based [63] architecture, following previous works [16], [17]. For proposal representations, two types are extracted, one is the positive proposal that represents the video segment corresponding to the sentence query, and the other is the negative intra-video proposal that represents the video segment that is not aligned to the sentence query.

Specifically, given a video and a sentence query, we first use a video backbone to obtain video features and a word embedding to obtain query embeddings. For the video, the pre-trained 3D Convolutional Neural Network [64] encodes segment-level video features. For the sentence query, the pre-trained GloVe [65] word embeddings are adopted. The query encoder adopts a transformer encoder structure [63]. To encode the global representation of the query features, we apply mean pooling over all word features to obtain the sentence-level query feature. Then, we utilize the proposal encoder, which is based on a transformer, to handle the multi-modal interaction between the video features and word features of the query, following CPL [16]. The proposal encoder outputs the proposal weights for end-to-end training. To encode the global representation of proposals, we pool the proposal features by computing the weighted sum of raw video features and their corresponding proposal weights. To discriminate the intra-video information, the proposal encoder encodes two types of proposals: the positive proposal and the negative intra-video proposal.

B. Mining Positive Samples

For each anchor sample, unlike previous approaches [45], [18], [19], [23], [16] regarding all remaining samples in the training set as negative, we mine positive samples from the remaining training set to capture sophisticated semantic correlations in the sample space. Specifically, given a training set with N samples, for each anchor sample $\mathcal{S}_i$ with sentence query $\mathcal{Q}_i$ and video $\mathcal{V}_i$, we divide the remaining training set samples into similar and dissimilar sets. we first adopt a pre-trained text encoder f, *i.e.*, SentenceTransformer [66], to extract the text features of the entire training set. Then, we compute the cosine similarity between the anchor text query and all remaining text queries in the training set, as

$$\text{Mat[i, j]} = \cos\big(f(\mathcal{Q}_i), f(\mathcal{Q}_j)\big). \tag{1}$$

The top-k most similar samples form a similar subset, while the remaining samples form a dissimilar subset, as

$$\mathcal{S}_i^{sim} = \left\{ (\mathcal{Q}_j, \mathcal{V}_j) \mid j \in \underset{j \neq i}{\text{Top-k-index}}\,(\text{Mat[i, j]}) \right\}, \tag{2}$$

$$\mathcal{S}_i^{dis} = \mathcal{S} \setminus \left(\{S_i\} \cup \mathcal{S}_i^{sim} \right). \tag{3}$$

The process for mining positive samples is outlined in Algorithm 1. Its runtime consists of two main components: query feature extraction with a complexity of $O(n)$ and the retrieval process with a complexity of $O(n^2)$. In practice, the retrieval phase demonstrates remarkable efficiency when

Algorithm 1 Mining Positive Samples

Input: N samples, each sample $\mathcal{S}_i$ has a query $\mathcal{Q}_i$ and a video $\mathcal{V}_i$
Output: Similar sample dictionary $\mathcal{S}^{sim}$, Dissimilar sample dictionary $\mathcal{S}^{dis}$
for $i = 1$ to N **do**
  Extract query feature $f(\mathcal{Q}_i)$
end for
for $i = 1$ to N **do**
  for $j = 1$ to N **do**
    Compute Cosine Similarity $\text{Mat}[i,j] = \cos\big(f(\mathcal{Q}_i), f(\mathcal{Q}_j)\big)$
  end for
  Get top-k indices $\text{Index}_i^{sim} = \text{Top-k-index}_{j \neq i}\,\text{Mat}[i,j]$
  Get similar sample set $\mathcal{S}_{sim}^{(i)} = \big\{(\mathcal{Q}_j, \mathcal{V}_j) \mid j \in \text{Index}_i^{sim}\big\}$
  Get dissimilar sample set $\mathcal{S}_{dis}^{(i)} = \mathcal{S} \setminus \Big\{\{\mathcal{S}_i\} \cup \mathcal{S}_{sim}^{(i)}\Big\}$
end for
Return Similar sample dictionary $\mathcal{S}_{sim}$ and Dissimilar sample dictionary $\mathcal{S}_{dis}$

leveraging PyTorch's highly-optimized vectorized operations (*i.e.,* topk), typically completing within one second for 10k-level samples. Moreover, as illustrated in Table IX, the time required by query feature extraction is usually less than 1% of the time for weakly supervised training, largely because the feature extraction is a pre-processing step requiring only one epoch, whereas WSTSG training involves multiple epochs.

Then, we randomly select a similar sample and a dissimilar sample from these two subsets for training, respectively.

Next, we input the anchor, similar, and dissimilar query-video pairs into the query and proposal encoders to extract their global representations, which consist of three parts. The first part is the query representations of similar and dissimilar samples, labeled as q_{sim} and q_{dis}. The second part is the positive proposal representations for the anchor, similar and dissimilar query-video pairs, labeled as p, p_{sim}, and p_{dis}. The final part is the negative intra-video proposal representation of the anchor sample, labeled as p_n. In summary, there are four types of proposal features: p, p_{sim}, p_{dis}, and p_n, as well as two types of query features: q_{sim} and q_{dis}. Then, all query and proposal features are L_2 normalized.

C. PSM-Guided Contrastive Loss

To distinguish between similar and dissimilar sample pairs for each anchor proposal, we propose a PSM-guided contrastive loss, which employs a margin loss to ensure that the cosine similarity between the anchor proposal and the similar sample is smaller than that between the anchor proposal and the dissimilar sample. The similar and dissimilar samples can be represented as two modalities: queries or proposals. Both the two-modal versions and the full form of PSM-guided contrastive losses are given as

$$\mathcal{L}_{query} = \max\big(p \cdot q_{dis} - p \cdot q_{sim} + \gamma_1, 0\big), \tag{4}$$

$$\mathcal{L}_{prop} = \max\big(p \cdot p_{dis} - p \cdot p_{sim} + \gamma_2, 0\big), \tag{5}$$

$$\mathcal{L}_{PSM}^{CL} = \mathcal{L}_{query} + \mathcal{L}_{prop}, \tag{6}$$

here, the symbol $\cdot$ represents the inner product, which represents the cosine similarity as these features are L_2 normalized. γ_1 and γ_2 are hyperparameters that control the margin between the cosine similarities of the anchor proposal with respect to the similar and dissimilar samples.

D. PSM-Guided Rank Loss

To distinguish between the anchor proposal and the negative intra-video proposal, we propose a PSM-guided rank loss, which adopts a margin loss to ensure that the distance between the anchor proposal and the similar sample is smaller than the distance between the negative intra-video proposal and the similar sample. The similar samples can be represented as two modalities: queries or proposals. We apply the PSM-guided contrastive loss to measure the distance between the similar sample and an intra-video proposal, *i.e.*, the anchor proposal or the negative intra-video proposal, because the PSM-guided contrastive loss and the distance between the similar sample and an intra-video proposal are positively correlated. That is, a lower PSM-guided contrastive loss indicates that the intra-video proposal is closer to similar samples. Specifically, the distances between the anchor proposal and similar query $d(p, q_{sim})$ and proposals $d(p, p_{sim})$ can be represented by the PSM-guided contrastive losses, which can be represented as

$$d(p, q_{sim}) = \mathcal{L}_{query}, \tag{7}$$

$$d(p, p_{sim}) = \mathcal{L}_{prop}. \tag{8}$$

Similarly, the distances between the negative intra-video proposal and similar query $d(p_n, q_{sim})$ and proposals $d(p_n, p_{sim})$ can also be represented by the PSM-guided contrastive losses, which are given as

$$d(p_n, q_{sim}) = \mathcal{L}_{query}^{n} = \max\big(p_n \cdot q_{dis} - p_n \cdot q_{sim} + \gamma_3, 0\big), \tag{9}$$

$$d(p_n, p_{sim}) = \mathcal{L}_{prop}^{n} = \max\big(p_n \cdot p_{dis} - p_n \cdot p_{sim} + \gamma_4, 0\big), \tag{10}$$

here, γ_3 and γ_4 are the margin values for the contrastive loss. Finally, both the two-modal versions and the full form of the PSM-guided rank losses are given as

$$\begin{aligned}\mathcal{L}_{rank}^{query} &= \max(d(p, q_{sim}) - d(p_n, q_{sim}) + \gamma_5, 0) \\ &= \max\big(\mathcal{L}_{query} - \mathcal{L}_{query}^{n} + \gamma_5, 0\big),\end{aligned} \tag{11}$$

$$\begin{aligned}\mathcal{L}_{rank}^{prop} &= \max(d(p, q_{sim}) - d(p_n, q_{sim}) + \gamma_6, 0) \\ &= \max\big(\mathcal{L}_{prop} - \mathcal{L}_{prop}^{n} + \gamma_6, 0\big),\end{aligned} \tag{12}$$

$$\mathcal{L}_{PSM}^{rank} = \mathcal{L}_{rank}^{query} + \mathcal{L}_{rank}^{prop}, \tag{13}$$

Where γ_5/γ_6 are hyperparameters that regulate the margin between the distances of the similar sample with respect to the anchor and negative intra-video proposals.

E. Training and Inference

During training, we optimize the network using the reconstruction-based loss $\mathcal{L}_{base}$ [23], [16], [17] along with our two PSM-guided losses $\mathcal{L}_{PSM}^{CL}$ and $\mathcal{L}_{PSM}^{rank}$, the overall training loss is given as

$$\mathcal{L}_{PSM} = \mathcal{L}_{base} + \mathcal{L}_{PSM}^{CL} + \mathcal{L}_{PSM}^{rank}. \tag{14}$$

To improve the recall rate of the anchor proposal, we also generate multiple anchor and negative intra-video proposal pairs following [16], [17]. Moreover, the loss is applied only to the anchor proposal with the smallest loss, *i.e.*, the anchor proposal with maximum confidence.

During inference, to select the top-1 proposal from multiple anchor proposals, we adopt the vote-based proposal selection scheme as in previous work [16]. To avoid additional inference costs for mining positive samples and computation of two PSM-guided losses, we adopt only the reconstruction-based loss $\mathcal{L}_{base}$ for voting among multiple anchor proposals. Therefore, our PSM scheme introduces no additional memory and evaluation cost during inference.

IV. Experimental Setup

We conduct extensive experiments to evaluate our PSM on two tasks: WSTSG and grounded VideoQA. The WSTSG benchmarks consist of Charades-STA [10] and Activitynet Captions [67]. The grounded VideoQA benchmark includes NExT-GQA [68], which consists of two sub-tasks: weakly supervised temporal sentence grounding and keyframe-based question answering tasks.

A. Datasets

- **Charades-STA** [10] contains 5.3k/1.3k videos of human daily indoor activities, and 10.6k/3.2k video-query pairs for training/testing. The average video length is 30 seconds. We report our results on the test split.
- **ActivityNet Captions** [67] contains 10.0k/4.9k/5.0k videos from YouTube, and 37.0k/17.5k/17.0k video-query pairs for training/validation/testing. The average video length is 118 seconds. Following previous methods [26], we use val_2 as the testing set.
- **NExT-GQA** [68] contains 3.9k/0.6k/1.0k daily life videos, and 34.1k/3.4k/5.5k question-answering pairs for training/validation/testing. Each QA pair in both validation and test sets is also annotated with an answer interval, while there is no answer interval annotation in the training set. The average video length is 44 seconds. Following [68], we report our results on the test split.

B. Evaluation Metrics

For the WSTSG dataset, we use two conventional evaluation metrics introduced in [10], which are R@n,IoU=m, and R@n,mIoU. The R@n,IoU=m denotes the percentage of having at least one of the top-n predicted temporal boundaries with temporal Intersection over Union (tIoU) larger than the threshold m. The R@n,mIoU is the mean value of the highest tIoU in the n predicted temporal boundaries.

For the grounded VideoQA task, we adopt mIoU along with three other metrics following [68], they are (1) mIoP: It estimates whether the predicted temporal window lies inside the grounding. (2) Acc@GQA: A new metric proposed in [68], which denotes the percentages of questions that are both correctly answered and also visually grounded (i.e., IoP$\geq$0.5). (3) Acc@QA: standard metrics for QA task. The R@n is set to R@1 by default.

C. Implementation Details

For the WSTSG task, we build the PSM framework based on PPS [17]. Following PPS [17], for video segment features, we use C3D features [64] in ActivityNet Captions dataset and I3D features [69] in Charades-STA dataset. For word embeddings, we adopt GloVe features [65]. We set the maximum number of video segments to 200 and the maximum length of the sentence query to 20. For the transformers, the number of transformer layers is 3 and the number of attention heads is 4. The dimension of both visual and textual features is set to 256. For the masked sentence query, we randomly mask 1/3 of the words. During training, we use the Adam optimizer with a learning rate of 0.0004 and a batch size of 32. For mining positive samples, the top 20 most similar samples are selected to form a similar sample subset. To minimize storage requirements, we store the indices of similar samples for each anchor sample rather than retaining the full data entries. For the PSM-guided contrastive loss and PSM-guided rank loss hyperparameters, we set them as $\gamma_1 = \gamma_2 = \gamma_3 = \gamma_4 = 0.5$, $\gamma_5 = \gamma_6 = 0.15$. The grounded VideoQA task includes two sub-tasks: WSTSG and keyframe-based QA. For the WSTSG part, we built our PSM framework based on the NG baseline [68], which adopts a similar Gaussian mask used in CPL [16]. For the keyframe-based QA model, following [68], we adopt two models: Temp[CLIP] [70] and FrozenBiLM [71]. We uniformly sample 32 frames for each video. For other training hypermeters, we follow [68]. All γ_i (i = 1 to 6) hyperparameters adopt the same values as those used in the WSTSG task. For mining positive samples, the top 20 most similar samples form a similar sample subset.

D. Experimental Results

We evaluate our method against state-of-the-art (SoTA) models on two WSTSG datasets: Charades-STA and ActivityNet Captions, as well as a grounded VideoQA dataset: NExT-GQA. For the WSTSG task, our comparisons include WSTSG models such as WSTAN [72], SCANet [81] and PPS [17]. The grounded VideoQA task includes two sub-tasks: WSTSG and keyframe-based QA. For the WSTSG sub-task, our comparisons include NG and NG+ [68]. For the keyframe-based QA sub-task, the VideoQA models include Temp [70] and FrozenBiLM [71]. Temp model uses multiple features, such as Swin [84], CLIP [85] and BLIP [86] features.

1) Comparison on Charades-STA and ActivityNet Captions: Table I and Table II present the comparative results on the Charades-STA and ActivityNet Captions datasets, respectively. The results indicate that our method consistently achieves the best or comparable performance across multiple recalls and

Methods	R@1,IoU=			R@5,IoU=		
	0.3	0.5	0.7	0.3	0.5	0.7
Random	20.12	8.61	3.39	68.42	37.57	14.98
CTF [8]	39.80	27.30	12.90	-	-	-
SCN [21]	42.96	23.58	9.97	95.56	71.80	38.87
WSTAN [72]	43.39	29.35	12.28	93.04	76.13	41.53
BAR [73]	44.97	27.04	12.23	-	-	-
MARN [22]	48.55	31.94	14.81	90.70	70.00	37.40
CCL [74]	-	33.21	15.68	-	73.50	41.87
RTBPN [75]	60.04	32.36	13.24	97.48	71.85	41.18
LoGAN [20]	51.67	34.68	14.54	92.74	74.30	39.11
CRM [19]	53.66	34.76	16.37	-	-	-
VCA [76]	58.58	38.13	19.57	98.08	78.75	37.75
LCNet [77]	59.60	39.19	18.87	94.78	80.56	45.24
CWSTG [78]	43.31	31.02	16.53	95.54	77.53	41.91
CPL [16]	66.40	49.24	22.39	96.99	84.71	52.37
CPI [79]	67.64	50.47	24.38	97.18	85.66	52.98
CCR [80]	68.59	50.79	23.75	96.85	84.48	52.44
SCANet [81]	68.04	50.85	24.07	98.24	86.32	53.28
UGS [47]	69.16	52.18	23.94	-	-	-
OmniD [82]	68.30	52.31	24.35	-	-	-
MMDist [83]	68.90	53.29	25.27	-	-	-
PPS [17]	69.06	51.49	26.16	99.18	86.23	53.01
Ours (PPS + PSM)	**71.89**	**54.36**	**28.73**	**99.19**	**88.35**	**55.87**

TABLE I: Performance comparisons on Charades-STA dataset. Bold and underlined numbers denote the best results and the second-best results, respectively.

Methods	R@1,IoU=			R@5,IoU=		
	0.1	0.3	0.5	0.1	0.3	0.5
Random	38.23	18.64	7.63	75.74	52.78	29.49
CTF [8]	74.20	44.30	23.60	-	-	-
SCN [21]	71.48	47.23	29.22	90.88	71.56	55.69
WSTAN [72]	79.78	52.45	30.01	93.15	79.38	63.42
BAR [73]	-	49.03	30.73	-	-	-
MARN [22]	-	47.01	29.95	-	72.02	57.49
CCL [74]	-	50.12	31.07	-	77.36	61.29
RTBPN [75]	73.73	49.77	29.63	93.89	79.89	60.56
VCA [76]	67.96	50.45	31.00	92.14	71.79	53.83
LCNet [77]	78.58	48.49	26.33	93.95	82.51	62.66
CWSTG [78]	71.86	46.62	29.52	93.75	80.92	66.61
CPL [16]	82.55	55.73	31.37	87.24	63.05	43.13
CCR [80]	80.32	53.21	30.39	91.44	71.97	56.50
SCANet [81]	**83.62**	56.07	31.52	94.36	82.34	64.09
CRM [19]	81.61	55.26	32.19	-	-	-
OmniD [82]	83.24	57.34	31.60	-	-	-
PPS [17]	81.84	59.29	31.25	95.28	85.54	71.32
MMDist [83]	83.11	58.69	32.52	-	-	-
UGS [47]	82.10	58.07	**36.91**	-	-	-
Ours (PPS + PSM)	83.25	**60.81**	33.64	**96.83**	**86.92**	**73.65**

TABLE II: Performance comparisons on ActivityNet Captions dataset. Bold and underlined numbers denote the best results and the second-best results, respectively.

IoU thresholds. Specifically, for Charades-STA dataset, our method (PPS + PSM) outperforms the state-of-the-art PPS [17] and SCANet [81] methods by margins of 2.83%, 2.87%, 2.57%, 2.03%, and 2.59% on R@1,IoU=0.3, R@1,IoU=0.5, R@1,IoU=0.7, R@5,IoU=0.5, and R@5,IoU=0.7, respectively. For ActivityNet Captions dataset, our method outperforms the state-of-the-art by 1.52%, 1.55%, 1.38%, and 2.33% on R@1,IoU=0.5, R@1,IoU=0.7, R@5,IoU=0.3, R@5,IoU=0.5, and R@5,IoU=0.7, respectively. These results highlight the proposals generated by our method has higher quality. The performance boost is primarily achieved by the discriminative supervision from positive samples. While UGS [47] achieves the best performance on R@1,IoU=0.7 for the ActivityNet Captions dataset, its model ensembling strategy relies on multiple reconstruction-based models to aggregate diverse confidence scores during inference, which suffers from reduced diversity in the generated proposals [47]. This drawback leads to inferior performance on R@1,IoU=0.3 and R@1,IoU=0.5 compared to our method. Moreover, the model ensembling strategy increases computational costs, demanding nearly twice the inference time of our method.

2) Comparison on NExT-GQA: To assess the effectiveness of PSM on the grounded VideoQA task, we conduct experiments on the NExT-GQA dataset, with results summarized in Table III. The experimental results indicate that our method (NG + PSM) achieves significant improvements on the NExT-GQA dataset with mIoP, mIoU, and Acc@GQA. Specifically, when using the Temp[CLIP] [70] as the VideoQA model, our method outperforms the state-of-the-art NG+ [68] method by 2.1%, 2.7%, and 1.9% on mIoP, mIoU, and Acc@GQA, respectively. Moreover, our method outperforms our baseline NG by 2.0%, 7.1%, and 2.4% on mIoP, mIoU, and Acc@GQA, respectively. When using the FrozenBiLM [71] as the VideoQA model, our method outperforms the state-of-the-art NG+ method by 1.7%, 3.3%, and 0.7% on mIoP, mIoU, and Acc@GQA, respectively. Note that NG+ requires additional annotations of GPT4 [87], whereas our approach achieves state-of-the-art performance without requiring any additional annotations, indicating the superiority of mining positive samples from other video samples. These results signify that our PSM effectively guides the VideoQA model to prioritize the correct temporal moments providing visual evidence. Moreover, our method achieves better QA accuracy with more precise visual evidence for both VideoQA baselines, *i.e.*, Temp[CLIP] and FrozenBiLM.

E. Ablation Study

We conduct extensive ablation experiments on the Charades-STA dataset to explore the effects of different factors, including different components of PSM, the sample mining strategy, the number of similar query-video pairs, the feature types for mining similar queries, different backbones, and hyperparameters. The experimental settings remain consistent with those defined earlier. The findings from these ablation studies provide more in-depth insights into the critical elements that contribute to the effectiveness of our proposed framework.

1) Effect of different components of PSM: We use the PPS baseline to ablate the following designs of PSM: PSM-guided contrastive loss L_{PSM}^{CL} and PSM-guided rank loss L_{PSM}^{rank}. Each has query and proposal modalities, resulting in four losses: $\mathcal{L}_{query}$, $\mathcal{L}_{prop}$, $\mathcal{L}_{query}^{rank}$, and $\mathcal{L}_{prop}^{rank}$. The results are shown in Table IV. Row 1 is the baseline of our model, which does not use positive sample mining. Among the combinations of the four losses, adopting all PSM-guided

WSTSG Method	QA Model	Vis Enc	Text Enc	Acc			IoP			IoU		
				QA	QA°	GQA	mIoP	0.3	0.5	mIoU	0.3	0.5
Human	-	-	-	93.3	-	82.1	72.1	91.7	86.2	61.2	86.9	70.3
Random	-	-	-	20.0	20.0	1.7	21.1	20.6	8.7	21.1	20.6	8.7
PH [68]	VGT [88]	RCNN [89]	BT [90]	50.9	53.8	12.7	24.7	26.0	24.6	3.0	4.2	1.4
	VIOLETv2 [91]	VSWT [92]	BT	52.9	57.2	12.8	23.6	25.1	23.3	3.1	4.3	1.3
	VGT	RCNN	RBT [93]	55.7	57.7	14.4	25.3	26.4	25.3	3.0	3.6	1.7
	Temp[Swin] [70]	SWT [84]	RBT	55.9	58.7	13.5	23.1	24.7	23.0	4.9	6.6	2.3
	Temp[CLIP]	ViT-B [94]	RBT	57.9	60.7	14.7	24.1	26.2	24.1	6.1	8.3	3.7
	Temp[BLIP]	ViT-B	RBT	58.5	61.5	14.9	25.0	27.8	25.3	6.9	10.0	4.5
	Temp[CLIP]	ViT-L	RBT	59.4	62.5	15.2	25.4	28.2	25.5	6.6	9.3	4.1
	FrozenBiLM [71]	ViT-L	DBT [95]	69.1	71.8	15.8	22.7	25.8	22.1	7.1	10.0	4.4
NG [68]	Temp[CLIP]	ViT-L	RBT	59.4	62.7	15.5	25.8	28.8	25.9	7.7	10.9	4.6
	FrozenBiLM	ViT-L	DBT	70.4	73.1	17.2	24.0	28.5	23.5	9.2	13.0	5.8
NG+ [68]	Temp[CLIP]	ViT-L	RBT	60.2	63.3	16.0	25.7	31.4	25.5	12.1	17.5	8.9
	FrozenBiLM	ViT-L	DBT	70.8	73.1	17.5	24.2	28.5	23.7	9.6	13.5	6.1
Ours (NG + PSM)	Temp[CLIP]	ViT-L	RBT	61.8	65.1	17.9	**27.8**	**34.6**	**26.7**	**14.8**	**20.5**	**9.7**
	FrozenBiLM	ViT-L	DBT	**72.1**	**74.5**	**18.2**	25.9	31.4	24.5	12.9	16.4	7.7

TABLE III: Grounded QA performance on the NExT-GQA test set. ○: original NExT-QA. BT: BERT. RBT: RoBERTa. DBT: DeBERTa-V2-XL. FT5: Flan-T5-XL. Random: always return the entire video duration as the grounding result.

Loss				R@1,IoU=		R@5,IoU=	
$\mathcal{L}_{query}$	$\mathcal{L}_{prop}$	$\mathcal{L}^{rank}_{query}$	$\mathcal{L}^{rank}_{prop}$	0.5	mIoU	0.5	mIoU
×	×	×	×	51.49	44.87	86.23	69.32
✓	×	×	×	52.01	45.39	87.09	69.79
×	✓	×	×	52.45	45.82	87.03	69.93
×	×	✓	×	52.64	46.02	87.04	70.02
×	×	×	✓	52.86	46.34	87.39	70.18
✓	✓	×	×	52.93	45.96	87.21	70.07
×	×	✓	✓	53.47	46.33	87.68	70.52
✓	×	✓	×	53.26	46.25	87.34	70.46
×	✓	×	✓	53.81	46.56	87.77	70.88
✓	✓	✓	✓	**54.36**	**46.92**	**88.35**	**71.05**

TABLE IV: Ablation study of different components for positive sample mining on the Charades-STA dataset.

losses yields the best performance. This suggests that leveraging more discriminative supervision from positive samples enables the generated positive proposals to better represent temporal locations. Besides, we conclude some observations based on the results: (1) From the comparison between row 2 to row 5 and row 6 to row 7, we can observe that both the PSM-guided contrastive losses $\mathcal{L}_{query}$/$\mathcal{L}_{prop}$ and PSM-guided rank losses $\mathcal{L}^{rank}_{query}$/$\mathcal{L}^{rank}_{prop}$ contribute to the improved performance compared to the baseline. Notably, by incorporating intra-video information, which contains richer fine-grained details that are harder for the model to learn, our PSM-guided rank losses effectively improve the model's capability and provide a larger boost. (2) From the comparison between row 8 to row 9, both the query and the proposal losses have complementary effects, as the two losses provide two modality views for moderate coupling. (3) From the comparison between row 2 to row 6, row 7 to row 8, the proposal losses $\mathcal{L}_{prop}$/$\mathcal{L}^{rank}_{prop}$ achieve greater improvements than the query losses $\mathcal{L}_{query}$/$\mathcal{L}^{rank}_{query}$. We hypothesize that this phenomenon can be attributed to the video proposal's richer informational content compared to the query, which offers more robust supervision signals for the learning process. These experimental findings collectively demonstrate the significance of each individual component in our proposed framework and highlight their complementary interactions in achieving the best results.

Sample Mining Strategy	R@1,IoU=		R@5,IoU=	
	0.5	mIoU	0.5	mIoU
None	51.49	44.87	86.23	69.32
Hard Negative Mining	51.85	45.02	86.72	69.49
Positive Mining (CR loss)	53.47	46.12	87.43	70.49
Positive Mining (Ours)	**54.36**	**46.92**	**88.35**	**71.05**

TABLE V: Ablation study of sample mining strategy. The experiment is conducted on the Charades-STA dataset.

2) Effect of sample mining strategy: We conduct ablation experiments on the Charades-STA dataset to validate our positive sample mining strategy. Specifically, we investigate two variant designs. 1) Hard Negative Mining (HNM): treating the mined similar samples as hard negative instead of positive during training. 2) positive mining with common rank loss (CR loss): we adopt cosine similarity as the distance between the similar sample and an intra-video proposal. Consequently, Equations 7, 8, 9 and 10 are modified. For example, Equation 7 is now defined as $d(p, q_{sim}) = p \cdot q_{sim}$. As shown in Table V, the HNM variant achieves only marginal performance gain (+0.15% for R@1,mIoU). We attribute this to the inherent design of the PPS baseline: negative intra-video proposals already serve as effective hard negatives through contrastive learning, making additional negative mining less impactful. For another, the CR loss variant only shows marginal performance over using PSM-guided contrastive loss alone (*e.g.,* 46.12% vs 45.96% in Table IV on R@1,mIoU), and underperforms our method. This result highlights the importance of both constraints to similar and dissimilar samples in PSM-guided rank loss, comparing to sole alignment to similar samples in

Similar Samples Number	R@1,IoU=		R@5,IoU=	
	0.5	mIoU	0.5	mIoU
0 (baseline)	51.49	44.87	86.23	69.32
1	52.78	45.69	87.48	70.43
3	53.41	46.06	87.96	70.76
5	53.88	46.49	88.03	70.65
10	54.20	46.88	88.29	70.96
20	**54.36**	46.92	**88.35**	**71.05**
30	54.32	**46.95**	88.31	**71.05**

TABLE VI: Ablation study of the number of similar samples for positive sample mining on the Charades-STA dataset.

Similar Query Feat.	R@1,IoU=		R@5,IoU=	
	0.5	mIoU	0.5	mIoU
Glove [mean]	53.35	46.54	87.32	70.43
BERT [mean]	53.97	46.80	87.88	70.69
BERT [CLS]	53.80	46.67	87.45	70.75
SentenceTransformer	**54.36**	**46.92**	**88.35**	**71.05**

TABLE VII: Ablation study of the feature types for mining similar queries in positive sample mining. The experiment is conducted on the Charades-STA dataset.

Method	+ PSM	R@1, IoU=		R@5,IoU=	
		0.5	mIoU	0.5	mIoU
CNM [23]	×	35.43	39.54	-	-
	✓	**37.69**	**41.43**	-	-
CPL [16]	×	49.24	42.91	84.71	67.66
	✓	**52.56**	**45.24**	**86.92**	**69.09**
PPS [17]	×	51.49	44.87	86.23	69.32
	✓	**54.36**	**46.92**	**88.35**	**71.05**

TABLE VIII: Results on the Charades-STA datasets when our PSM is applied on different backbone networks. Our PSM significantly boosts the performance of the existing networks.

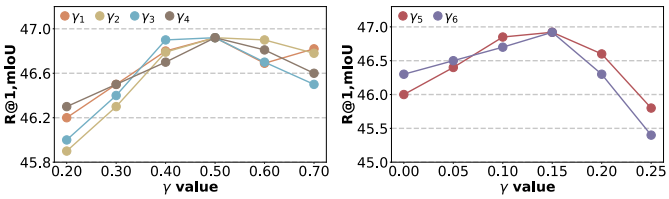

Fig. 4: Ablation study by varying γ_1 to γ_6 for positive sample mining on the Charades-STA dataset. When varying each γ_i, the remaining γ values are fixed.

the CR loss variant.

3) Effect of the number of similar samples: We conduct a comprehensive ablation study to assess the impact of the number of similar samples for positive sample mining on model performance, with the results detailed in Table VI. We observe the following findings: (1) Using various number of similar samples achieves better results compared to the baseline using no similar sample, even when utilizing only a single similar sample. This highlights the importance of leveraging positive samples as more discriminative supervision signals in the learning process. (2) As evidenced in the last two rows of Table VI, the performance gradually saturates as the number of similar samples exceeds a certain threshold. This phenomenon can be explained by the inherent trade-off in mining positive samples: while increasing the number of similar samples can increase diversity, it also inevitably introduces dissimilar samples into the subset of similar samples, which could potentially compromise the model's performance.

4) Effect of feature types for mining similar queries: The choice of similar samples is critical to the effectiveness of PSM, as it directly affects the model's ability to capture sophisticated semantic correlations in the sample space. To investigate this, we choose multiple textual models to retrieve similar queries, including word-level features from GloVe and BERT, as well as sentence-level features from BERT's [CLS] token and SentenceTransformer. For word-level features, we apply mean pooling on the word-level features to obtain the sentence-level representations. Subsequently, all sentence-level features are used to select top-k similar query-video pairs. The final WSTSG results are presented in Table VII. Our method with the SentenceTransformer features yields the best results, while our method with the GloVe features performs the worst. We hypothesize that the GloVe features exhibit limited discriminative capability, as evidenced by the cosine similarity matrix of the entire Charades-STA dataset, which ranges narrowly from 0.7 to 1. In contrast, the SentenceTransformer features show a much broader distribution, with cosine similarity values spanning the full range from -1 to 1.

5) Effects of different backbones: To evaluate the generalizability of PSM, we build PSM upon multiple backbones, including CNM [23], CPL [16], and PPS [17]. Table VIII reports the results of this ablation study in terms of R@1, IoU=0.5, and mIoU for both R@1 and R@5 metrics. Specifically, in terms of R@1, IoU=0.5, PSM improves performance by 2.26 for CNM, 3.32 for CPL, and 2.87 for PPS. For R@1, mIoU, PSM leads to gains of 1.89 for CNM, 2.33 for CPL, and 2.05 for PPS. These results highlight the versatility and effectiveness of our PSM in enhancing the performance of different backbones on the WSTSG task. The consistent improvements across all evaluation metrics confirm that our method can be seamlessly integrated into existing networks to achieve better results. The performance of CNM at R@5 is not provided, as CNM only generates one anchor proposal. As demonstrated in Table VIII, our PSM exhibits more substantial performance gains when integrated with CPL and PPS compared to CNM. This enhanced performance can be attributed to the inherent advantages of CPL and PPS, which generate multiple anchor proposals and selectively optimize the proposal with the highest confidence score. This multi-proposal approach inherently provides greater robustness than the single-anchor-proposal framework CNM.

6) Effect of hyperparameters: We conduct comprehensive experiments to evaluate the impact of different combinations of hyperparameters for the PSM-guided contrastive loss and the PSM-guided rank loss. Specifically, we evaluate $\gamma_1, \gamma_2, \gamma_3$ and γ_4 for the PSM-guided contrastive loss and γ_5 and γ_6 for the PSM-guided rank loss. When varying each γ_i, the remaining γ

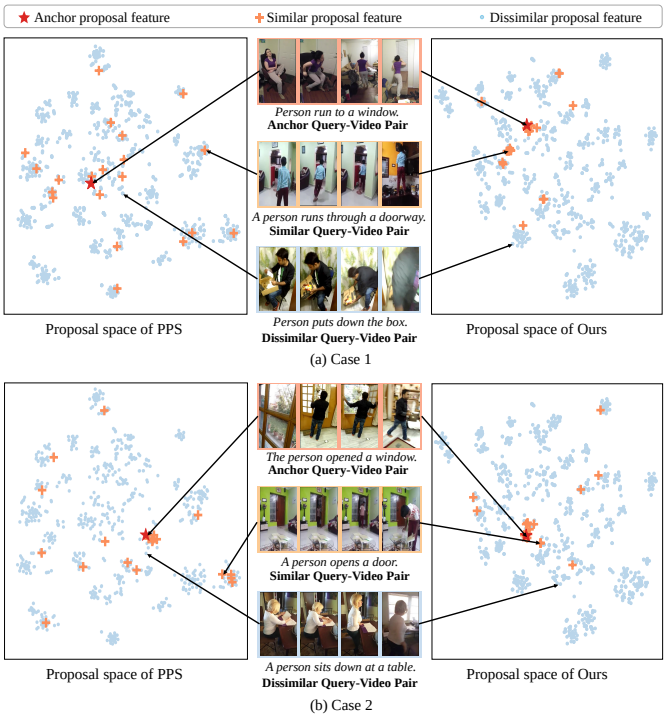

Fig. 5: The t-SNE results of the proposal spaces encoded by baseline PPS and our method (PPS + PSM) on the Charades-STA dataset. Two test samples are randomly selected. For each anchor sample, we present one similar and one dissimilar sample for visualization.

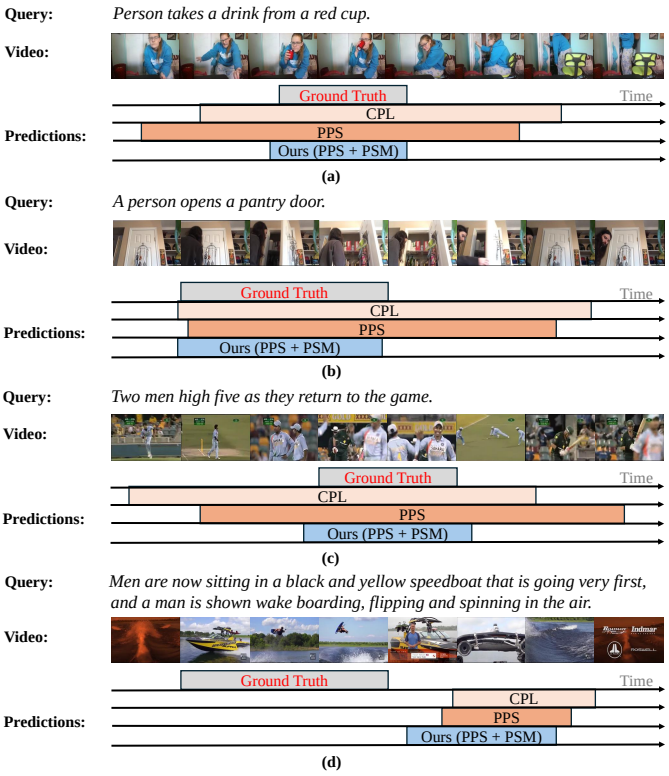

Fig. 6: Qualitative examples of the ground truth, the baselines CPL [16] and PPS [17], as well as our method (PPS + PSM). Examples (a, b) are from the Charades-STA dataset, and (c, d) are from the ActivityNet Captions dataset.

values are fixed. The results are illustrated in Fig. 4. Through this ablation study, we observe several important findings: (1) the combination of margins ($\gamma_1 = \gamma_2 = \gamma_3 = \gamma_4 = 0.5, \gamma_5 = \gamma_6 = 0.15$) results in the optimal performance. (2) The model is less sensitive to the variations in $\gamma_1, \gamma_2, \gamma_3, \gamma_4$ than to changes in γ_5, γ_6. (3) The performance significantly degrades when γ_5 and γ_6 deviate from their optimal values, with both extremely small and large values. We hypothesize that when these values are too small, the model struggles to distinguish between the anchor proposal and the negative intra-video proposal, which is crucial for WSTSG [16]. On the other hand, when γ_5 and γ_6 are too large, we observe that the model is difficult to optimize in the early training stage, as the initial predictions are much more noisy.

F. Qualitative Analysis

To validate that our PSM effectively captures the correlations between the anchor samples and similar samples, we visualize the encoded proposal space using the Charades-STA dataset. Specifically, two anchor samples are randomly selected and their corresponding top 20 most similar samples are identified. Then, we employ t-SNE [96] to visualize the proposal features encoded by PPS [17] and our method (PPS + PSM). From Fig. 5, we observe that the similar proposal features encoded by PPS are sparsely distributed, and fail to form a clear clustering around the anchor proposal feature. This indicates that PPS is ineffective in grouping proposals with semantics similar to the anchor proposal. In contrast, the similar proposal features encoded by our method are tightly clustered around the anchor proposal feature, highlighting our PSM's capability to preserve the semantic similarity within the proposal space. However, for certain query-video pairs, the video clips corresponding to the queries may exhibit complex semantics, where multiple events occur simultaneously. This complexity poses challenges in accurately establishing precise proposals. As a result, some similar proposal features encoded by our method may deviate from the anchor proposal feature.

Fig. 6 shows the qualitative comparison of the results generated by two baselines and our method (PPS + PSM). From this figure, we make the following observations: (1) From Fig. 6(a) (b), and (c), it is notable that our method can achieve better results than these baselines, proving that our PSM technique can capture more accurate query-relevant temporal locations. (2) As shown in Fig. 6(a), (b), and (c), CPL and PPS tend to produce longer proposals, while our method can remove the irrelevant proposals near the ground-truth proposals. This is mainly because our method mines similar samples from the training set and requires maintaining correlations between the anchor sample and the similar samples. As the proposal length increases, maintaining these correlations becomes more challenging due to the inclusion of irrelevant temporal context, which complicates the feature alignment process. (3) Fig. 6(d) shows that the compared methods and our method perform poorly when the query is highly complex. This performance limitation can be attributed to the

Dataset	Charades-STA	ActivityNet Captions
Training Size	10.6k	37.4k
Feature Extraction Time (MPS)	3s	13s
Retrieval Time (MPS)	0.07s	0.58s
WSTSG Training Time	1867s	7601s
Total Time	1870s	7615s

TABLE IX: Training cost distribution for positive sample mining. Here MPS represents mining positive samples. The experiment is conducted on an A100 GPU.

inherent challenge of identifying sufficiently similar queries in the training set for the complex anchor queries, resulting in weakened discriminative supervision signals from the remaining training samples, ultimately hindering the model's capacity to capture sophisticated correlations between query-video samples.

We also give a training cost distribution for our method (PPS + PSM) on an A100 GPU. The result is shown in Table IX. We can observe that the feature extraction time and retrieval time of mining positive samples are minimal when compared to the WSTSG training time. The retrieval phase demonstrates remarkable efficiency since we leverage PyTorch's highly-optimized vectorized operations (*i.e.,* topk). On the other hand, the feature extraction speed is fast because the feature extraction is a pre-processing step requiring only one epoch, whereas WSTSG training involves multiple epochs.

V. Conclusions and Future Directions

In this work, we propose the first positive-sample-based method for WSTSG. We mine positive samples for each anchor sample and leverage them as more discriminative supervision. Moreover, we propose a PSM-guided contrastive loss to discriminate similar and dissimilar samples. Additionally, we design a PSM-guided rank loss to improve the distinction between the anchor proposal and the negative intra-video proposal. Qualitative and quantitative experiments on two tasks, WSTSG and grounded VideoQA, demonstrate the superior performance of PSM. Extensive ablation studies further validate the effectiveness of PSM.

While PSM demonstrates substantial improvements in the WSTSG task, it has some limitations. First, PSM requires additional training costs for mining similar samples and loss computation. Secondly, when the video clips corresponding to the queries contain complex semantics, where multiple events occur simultaneously, it is challenging for our model to output precise proposals. Thirdly, our method mines similar samples based on the global semantics of the sentence query, which can be difficult to find similar samples for complex queries. This limitation could potentially be addressed through the decomposition of complex queries into distinct sub-events, and employing a more granular retrieval process that operates on these individual sub-event components, rather than attempting to match entire queries.

VI. Acknowledgements

This work was supported by the National Key R&D Program of China(NO.2022ZD0160505) and Industry Collaboration Projects Grant, Shanghai Committee of Science and Technology, China (Grant No.22YF1461500).

References

[1] Ke Zhang, Wei-Lun Chao, Fei Sha, and Kristen Grauman. Video summarization with long short-term memory. In *European Conference on Computer Vision*, pages 766–782, 2016.

[2] Mrigank Rochan, Linwei Ye, and Yang Wang. Video summarization using fully convolutional sequence networks. In *Proceedings of the European Conference on Computer Vision (ECCV)*, pages 347–363, 2018.

[3] Yifei Huang, Guo Chen, Jilan Xu, Mingfang Zhang, Lijin Yang, Baoqi Pei, Hongjie Zhang, Lu Dong, Yali Wang, Limin Wang, et al. Egoexolearn: A dataset for bridging asynchronous ego-and exo-centric view of procedural activities in real world. In *Proceedings of the IEEE Conference on Computer Vision and Pattern Recognition*, pages 22072–22086, 2024.

[4] Jianfeng Dong, Xirong Li, Chaoxi Xu, Shouling Ji, Yuan He, Gang Yang, and Xun Wang. Dual encoding for zero-example video retrieval. In *Proceedings of the IEEE/CVF Conference on Computer Vision and Pattern Recognition*, pages 9346–9355, 2019.

[5] Valentin Gabeur, Chen Sun, Karteek Alahari, and Cordelia Schmid. Multi-modal transformer for video retrieval. In *European Conference on Computer Vision*, pages 214–229, 2020.

[6] Xiaohan Wang, Linchao Zhu, and Yi Yang. T2vlad: global-local sequence alignment for text-video retrieval. In *Proceedings of the IEEE/CVF Conference on Computer Vision and Pattern Recognition*, pages 5079–5088, 2021.

[7] Yifei Huang, Minjie Cai, Zhenqiang Li, Feng Lu, and Yoichi Sato. Mutual context network for jointly estimating egocentric gaze and action. *IEEE Transactions on Image Processing*, 29:7795–7806, 2020.

[8] Zhenfang Chen, Lin Ma, Wenhan Luo, Peng Tang, and Kwan-Yee K Wong. Look closer to ground better: Weakly-supervised temporal grounding of sentence in video. *arXiv preprint arXiv:2001.09308*, 2020.

[9] Yifei Huang, Minjie Cai, Zhenqiang Li, and Yoichi Sato. Predicting gaze in egocentric video by learning task-dependent attention transition. In *Proceedings of the European Conference on Computer Vision*, 2018.

[10] Jiyang Gao, Chen Sun, Zhenheng Yang, and Ram Nevatia. Tall: Temporal activity localization via language query. In *Proceedings of the IEEE International Conference on Computer Vision*, pages 5267–5275, 2017.

[11] Shaoning Xiao, Long Chen, Songyang Zhang, Wei Ji, Jian Shao, Lu Ye, and Jun Xiao. Boundary proposal network for two-stage natural language video localization. In *Proceedings of the AAAI Conference on Artificial Intelligence*, volume 35, pages 2986–2994, 2021.

[12] Kevin Qinghong Lin, Pengchuan Zhang, Joya Chen, Shraman Pramanick, Difei Gao, Alex Jinpeng Wang, Rui Yan, and Mike Zheng Shou. Univtg: Towards unified video-language temporal grounding. In *Proceedings of the IEEE/CVF International Conference on Computer Vision*, pages 2794–2804, 2023.

[13] Runzhou Ge, Jiyang Gao, Kan Chen, and Ram Nevatia. Mac: Mining activity concepts for language-based temporal localization. In *2019 IEEE Winter Conference on Applications of Computer Vision (WACV)*, pages 245–253. IEEE, 2019.

[14] Songyang Zhang, Houwen Peng, Jianlong Fu, and Jiebo Luo. Learning 2d temporal adjacent networks for moment localization with natural language. In *Proceedings of the AAAI Conference on Artificial Intelligence*, volume 34, pages 12870–12877, 2020.

[15] Qi Zheng, Jianfeng Dong, Xiaoye Qu, Xun Yang, Yabing Wang, Pan Zhou, Baolong Liu, and Xun Wang. Progressive localization networks for language-based moment localization. *ACM Transactions on Multimedia Computing, Communications and Applications*, 19(2):1–21, 2023.

[16] Minghang Zheng, Yanjie Huang, Qingchao Chen, Yuxin Peng, and Yang Liu. Weakly supervised temporal sentence grounding with gaussian-based contrastive proposal learning. In *Proceedings of the IEEE/CVF Conference on Computer Vision and Pattern Recognition*, pages 15555–15564, 2022.

[17] Sunoh Kim, Jungchan Cho, Joonsang Yu, YoungJoon Yoo, and Jin Young Choi. Gaussian mixture proposals with pull-push learning scheme to capture diverse events for weakly supervised temporal video grounding. In *Proceedings of the AAAI Conference on Artificial Intelligence*, volume 38, pages 2795–2803, 2024.

[18] Mingfei Gao, Larry S Davis, Richard Socher, and Caiming Xiong. Wslln: Weakly supervised natural language localization networks. *arXiv preprint arXiv:1909.00239*, 2019.

[19] Jiabo Huang, Yang Liu, Shaogang Gong, and Hailin Jin. Cross-sentence temporal and semantic relations in video activity localisation. In *Proceedings of the IEEE/CVF International Conference on Computer Vision*, pages 7199–7208, 2021.

[20] Reuben Tan, Huijuan Xu, Kate Saenko, and Bryan A Plummer. Logan: Latent graph co-attention network for weakly-supervised video moment

retrieval. In *Proceedings of the IEEE/CVF Winter Conference on Applications of Computer Vision*, pages 2083–2092, 2021.

[21] Zhijie Lin, Zhou Zhao, Zhu Zhang, Qi Wang, and Huasheng Liu. Weakly-supervised video moment retrieval via semantic completion network. In *Proceedings of the AAAI Conference on Artificial Intelligence*, volume 34, pages 11539–11546, 2020.

[22] Yijun Song, Jingwen Wang, Lin Ma, Zhou Yu, and Jun Yu. Weakly-supervised multi-level attentional reconstruction network for grounding textual queries in videos. *arXiv preprint arXiv:2003.07048*, 2020.

[23] Minghang Zheng, Yanjie Huang, Qingchao Chen, and Yang Liu. Weakly supervised video moment localization with contrastive negative sample mining. In *Proceedings of the AAAI Conference on Artificial Intelligence*, volume 36, pages 3517–3525, 2022.

[24] Lisa Anne Hendricks, Oliver Wang, Eli Shechtman, Josef Sivic, Trevor Darrell, and Bryan Russell. Localizing moments in video with natural language. In *Proceedings of the IEEE International Conference on Computer Vision*, pages 5803–5812, 2017.

[25] Bin Jiang, Xin Huang, Chao Yang, and Junsong Yuan. Cross-modal video moment retrieval with spatial and language-temporal attention. In *Proceedings of the 2019 on International Conference on Multimedia Retrieval*, pages 217–225, 2019.

[26] Jingyuan Chen, Xinpeng Chen, Lin Ma, Zequn Jie, and Tat-Seng Chua. Temporally grounding natural sentence in video. In *Proceedings of the 2018 Conference on Empirical Methods in Natural Language Processing*, pages 162–171, 2018.

[27] Yitian Yuan, Lin Ma, Jingwen Wang, Wei Liu, and Wenwu Zhu. Semantic conditioned dynamic modulation for temporal sentence grounding in videos. *Advances in Neural Information Processing Systems*, 32, 2019.

[28] Zongmeng Zhang, Xianjing Han, Xuemeng Song, Yan Yan, and Liqiang Nie. Multi-modal interaction graph convolutional network for temporal language localization in videos. *IEEE Transactions on Image Processing*, 30:8265–8277, 2021.

[29] Hao Zhou, Chongyang Zhang, Yan Luo, Chuanping Hu, and Wenjun Zhang. Thinking inside uncertainty: Interest moment perception for diverse temporal grounding. *IEEE Transactions on Circuits and Systems for Video Technology*, 32(10):7190–7203, 2022.

[30] Yuelin Hu, Yuanwu Xu, Yuejie Zhang, Rui Feng, Tao Zhang, Xuequan Lu, and Shang Gao. Camg: Context-aware moment graph network for multimodal temporal activity localization via language. In *CCF International Conference on Natural Language Processing and Chinese Computing*, pages 429–441, 2023.

[31] Xin Sun, Jialin Gao, Yizhe Zhu, Xuan Wang, and Xi Zhou. Video moment retrieval via comprehensive relation-aware network. *IEEE Transactions on Circuits and Systems for Video Technology*, 33(9):5281–5295, 2023.

[32] Xuemei Zhang, Peng Zhao, Jinsheng Ji, Xiankai Lu, and Yilong Yin. Video corpus moment retrieval via deformable multi granularity feature fusion and adversarial training. *IEEE Transactions on Circuits and Systems for Video Technology*, 2023.

[33] Zhaobo Qi, Yibo Yuan, Xiaowen Ruan, Shuhui Wang, Weigang Zhang, and Qingming Huang. Collaborative debias strategy for temporal sentence grounding in video. *IEEE Transactions on Circuits and Systems for Video Technology*, 2024.

[34] Mayu Otani, Yuta Nakashima, Esa Rahtu, and Janne Heikkilä. Uncovering hidden challenges in query-based video moment retrieval. *arXiv preprint arXiv:2009.00325*, 2020.

[35] Can Zhang, Meng Cao, Dongming Yang, Jie Chen, and Yuexian Zou. Cola: Weakly-supervised temporal action localization with snippet contrastive learning. In *Proceedings of the IEEE/CVF Conference on Computer Vision and Pattern Recognition*, pages 16010–16019, 2021.

[36] Binglu Wang, Xun Zhang, and Yongqiang Zhao. Exploring sub-action granularity for weakly supervised temporal action localization. *IEEE Transactions on Circuits and Systems for Video Technology*, 32(4):2186–2198, 2021.

[37] Yufan Hu, Jie Fu, Mengyuan Chen, Junyu Gao, Jianfeng Dong, Bin Fan, and Hongmin Liu. Learning proposal-aware re-ranking for weakly-supervised temporal action localization. *IEEE Transactions on Circuits and Systems for Video Technology*, 34(1):207–220, 2023.

[38] Songchun Zhang and Chunhui Zhao. Cross-video contextual knowledge exploration and exploitation for ambiguity reduction in weakly supervised temporal action localization. *IEEE Transactions on Circuits and Systems for Video Technology*, 2023.

[39] Yibo Zhao, Hua Zhang, Zan Gao, Weili Guan, Meng Wang, and Shengyong Chen. A snippets relation and hard-snippets mask network for weakly-supervised temporal action localization. *IEEE Transactions on Circuits and Systems for Video Technology*, 2024.

[40] Liqi Yan, Qifan Wang, Siqi Ma, Jingang Wang, and Changbin Yu. Solve the puzzle of instance segmentation in videos: A weakly supervised framework with spatio-temporal collaboration. *IEEE Transactions on Circuits and Systems for Video Technology*, 33(1):393–406, 2022.

[41] ZHANG Yinhui, HAI Weiqi, HE Zifen, HUANG Ying, and CHEN Dongdong. Weakly supervised video instance segmentation with scale adaptive generation regulation. *Optics and Precision Engineering*, 31(18):2736–2751, 2023.

[42] Zhen Yang, Yuanfang Guo, Junfu Wang, Di Huang, Xiuguo Bao, and Yunhong Wang. Towards video anomaly detection in the real world: A binarization embedded weakly-supervised network. *IEEE Transactions on Circuits and Systems for Video Technology*, 2023.

[43] Peng Wu, Xuerong Zhou, Guansong Pang, Lingru Zhou, Qingsen Yan, Peng Wang, and Yanning Zhang. Vadclip: Adapting vision-language models for weakly supervised video anomaly detection. In *Proceedings of the AAAI Conference on Artificial Intelligence*, volume 38, pages 6074–6082, 2024.

[44] Yixuan Zhou, Yi Qu, Xing Xu, Fumin Shen, Jingkuan Song, and Heng Tao Shen. Batchnorm-based weakly supervised video anomaly detection. *IEEE Transactions on Circuits and Systems for Video Technology*, 2024.

[45] Niluthpol Chowdhury Mithun, Sujoy Paul, and Amit K Roy-Chowdhury. Weakly supervised video moment retrieval from text queries. In *Proceedings of the IEEE/CVF Conference on Computer Vision and Pattern Recognition*, pages 11592–11601, 2019.

[46] Minuk Ma, Sunjae Yoon, Junyeong Kim, Youngjoon Lee, Sunghun Kang, and Chang D Yoo. Vlanet: Video-language alignment network for weakly-supervised video moment retrieval. In *European Conference on Computer Vision*, pages 156–171, 2020.

[47] Yifei Huang, Lijin Yang, and Yoichi Sato. Weakly supervised temporal sentence grounding with uncertainty-guided self-training. In *Proceedings of the IEEE/CVF Conference on Computer Vision and Pattern Recognition*, pages 18908–18918, 2023.

[48] SouYoung Jin, Aruni RoyChowdhury, Huaizu Jiang, Ashish Singh, Aditya Prasad, Deep Chakraborty, and Erik Learned-Miller. Unsupervised hard example mining from videos for improved object detection. In *Proceedings of the European Conference on Computer Vision (ECCV)*, pages 307–324, 2018.

[49] Joshua Robinson, Ching-Yao Chuang, Suvrit Sra, and Stefanie Jegelka. Contrastive learning with hard negative samples. *arXiv preprint arXiv:2010.04592*, 2020.

[50] Hao Zhang, Aixin Sun, Wei Jing, Guoshun Nan, Liangli Zhen, Joey Tianyi Zhou, and Rick Siow Mong Goh. Video corpus moment retrieval with contrastive learning. In *Proceedings of the 44th International ACM SIGIR Conference on Research and Development in Information Retrieval*, pages 685–695, 2021.

[51] Sunjae Yoon, Ji Woo Hong, Eunseop Yoon, Dahyun Kim, Junyeong Kim, Hee Suk Yoon, and Chang D Yoo. Selective query-guided debiasing for video corpus moment retrieval. In *European Conference on Computer Vision*, pages 185–200. Springer, 2022.

[52] Sunjae Yoon, Ji Woo Hong, Soohwan Eom, Hee Suk Yoon, Eunseop Yoon, Daehyeok Kim, Junyeong Kim, Chanwoo Kim, and Chang D Yoo. Counterfactual two-stage debiasing for video corpus moment retrieval. In *ICASSP 2023-2023 IEEE International Conference on Acoustics, Speech and Signal Processing (ICASSP)*, pages 1–5. IEEE, 2023.

[53] Xiaohan Lan, Yitian Yuan, Hong Chen, Xin Wang, Zequn Jie, Lin Ma, Zhi Wang, and Wenwu Zhu. Curriculum multi-negative augmentation for debiased video grounding. In *Proceedings of the AAAI Conference on Artificial Intelligence*, volume 37, pages 1213–1221, 2023.

[54] Zhaobo Qi, Yibo Yuan, Xiaowen Ruan, Shuhui Wang, Weigang Zhang, and Qingming Huang. Bias-conflict sample synthesis and adversarial removal debias strategy for temporal sentence grounding in video. In *Proceedings of the AAAI Conference on Artificial Intelligence*, volume 38, pages 4533–4541, 2024.

[55] Sunoh Kim, Daeho Um, HyunJun Choi, and Jin Young Choi. Learnable negative proposals using dual-signed cross-entropy loss for weakly supervised video moment localization. In *Proceedings of the 32nd ACM International Conference on Multimedia*, pages 5318–5327, 2024.

[56] Hui Wu, Min Wang, Wengang Zhou, Houqiang Li, and Qi Tian. Contextual similarity distillation for asymmetric image retrieval. In *Proceedings of the IEEE/CVF Conference on Computer Vision and Pattern Recognition*, pages 9489–9498, 2022.

[57] Pavel Suma, Giorgos Kordopatis-Zilos, Ahmet Iscen, and Giorgos Tolias. Ames: Asymmetric and memory-efficient similarity estimation for instance-level retrieval. In *European Conference on Computer Vision*, pages 307–325, 2025.

[58] Yi Xie, Yihong Lin, Wenjie Cai, Xuemiao Xu, Huaidong Zhang, Yong Du, and Shengfeng He. D3still: Decoupled differential distillation for

asymmetric image retrieval. In *Proceedings of the IEEE/CVF Conference on Computer Vision and Pattern Recognition*, pages 17181–17190, 2024.

[59] Ivan Titov. Domain adaptation by constraining inter-domain variability of latent feature representation. In *proceedings of the 49th annual meeting of the Association for Computational Linguistics: Human language technologies*, pages 62–71, 2011.

[60] Yifan Wang, Lin Zhang, Ran Song, Hongliang Li, Paul L Rosin, and Wei Zhang. Exploiting inter-sample affinity for knowability-aware universal domain adaptation. *International Journal of Computer Vision*, 132(5):1800–1816, 2024.

[61] Mingfei Han, Yali Wang, Xiaojun Chang, and Yu Qiao. Mining inter-video proposal relations for video object detection. In *European Conference on Computer Vision*, pages 431–446, 2020.

[62] Qiang Qi, Zhenyu Qiu, Yan Yan, Yang Lu, and Hanzi Wang. Imc-det: Intra–inter modality contrastive learning for video object detection. *International Journal of Computer Vision*, pages 1–20, 2024.

[63] A Vaswani. Attention is all you need. *Advances in Neural Information Processing Systems*, 2017.

[64] Du Tran, Lubomir Bourdev, Rob Fergus, Lorenzo Torresani, and Manohar Paluri. Learning spatiotemporal features with 3d convolutional networks. In *Proceedings of the IEEE International Conference on Computer Vision*, pages 4489–4497, 2015.

[65] Jeffrey Pennington, Richard Socher, and Christopher D Manning. Glove: Global vectors for word representation. In *Proceedings of the 2014 Conference on Empirical Methods in Natural Language Processing (EMNLP)*, pages 1532–1543, 2014.

[66] Nils Reimers and Iryna Gurevych. Sentence-bert: Sentence embeddings using siamese bert-networks. In *Proceedings of the 2019 Conference on Empirical Methods in Natural Language Processing*. Association for Computational Linguistics, 11 2019.

[67] Ranjay Krishna, Kenji Hata, Frederic Ren, Li Fei-Fei, and Juan Carlos Niebles. Dense-captioning events in videos. In *Proceedings of the IEEE International Conference on Computer Vision*, pages 706–715, 2017.

[68] Junbin Xiao, Angela Yao, Yicong Li, and Tat-Seng Chua. Can i trust your answer? visually grounded video question answering. In *Proceedings of the IEEE/CVF Conference on Computer Vision and Pattern Recognition*, pages 13204–13214, 2024.

[69] Joao Carreira and Andrew Zisserman. Quo vadis, action recognition? a new model and the kinetics dataset. In *proceedings of the IEEE Conference on Computer Vision and Pattern Recognition*, pages 6299–6308, 2017.

[70] Shyamal Buch, Cristóbal Eyzaguirre, Adrien Gaidon, Jiajun Wu, Li Fei-Fei, and Juan Carlos Niebles. Revisiting the" video" in video-language understanding. In *Proceedings of the IEEE/CVF Conference on Computer Vision and Pattern Recognition*, pages 2917–2927, 2022.

[71] Antoine Yang, Antoine Miech, Josef Sivic, Ivan Laptev, and Cordelia Schmid. Zero-shot video question answering via frozen bidirectional language models. *Advances in Neural Information Processing Systems*, 35:124–141, 2022.

[72] Yuechen Wang, Jiajun Deng, Wengang Zhou, and Houqiang Li. Weakly supervised temporal adjacent network for language grounding. *IEEE Transactions on Multimedia*, 24:3276–3286, 2021.

[73] Jie Wu, Guanbin Li, Xiaoguang Han, and Liang Lin. Reinforcement learning for weakly supervised temporal grounding of natural language in untrimmed videos. In *Proceedings of the 28th ACM International Conference on Multimedia*, pages 1283–1291, 2020.

[74] Zhu Zhang, Zhou Zhao, Zhijie Lin, Xiuqiang He, et al. Counterfactual contrastive learning for weakly-supervised vision-language grounding. *Advances in Neural Information Processing Systems*, 33:18123–18134, 2020.

[75] Zhu Zhang, Zhijie Lin, Zhou Zhao, Jieming Zhu, and Xiuqiang He. Regularized two-branch proposal networks for weakly-supervised moment retrieval in videos. In *Proceedings of the 28th ACM International Conference on Multimedia*, pages 4098–4106, 2020.

[76] Zheng Wang, Jingjing Chen, and Yu-Gang Jiang. Visual co-occurrence alignment learning for weakly-supervised video moment retrieval. In *Proceedings of the 29th ACM International Conference on Multimedia*, pages 1459–1468, 2021.

[77] Wenfei Yang, Tianzhu Zhang, Yongdong Zhang, and Feng Wu. Local correspondence network for weakly supervised temporal sentence grounding. *IEEE Transactions on Image Processing*, 30:3252–3262, 2021.

[78] Jiaming Chen, Weixin Luo, Wei Zhang, and Lin Ma. Explore inter-contrast between videos via composition for weakly supervised temporal sentence grounding. In *Proceedings of the AAAI Conference on Artificial Intelligence*, volume 36, pages 267–275, 2022.

[79] Shuhan Kong, Liang Li, Beichen Zhang, Wenyu Wang, Bin Jiang, Chenggang Yan, and Changhao Xu. Dynamic contrastive learning with pseudo-samples intervention for weakly supervised joint video mr and hd. In *Proceedings of the 31st ACM International Conference on Multimedia*, pages 538–546, 2023.

[80] Zezhong Lv, Bing Su, and Ji-Rong Wen. Counterfactual cross-modality reasoning for weakly supervised video moment localization. In *Proceedings of the 31st ACM International Conference on Multimedia*, pages 6539–6547, 2023.

[81] Sunjae Yoon, Gwanhyeong Koo, Dahyun Kim, and Chang D Yoo. Scanet: Scene complexity aware network for weakly-supervised video moment retrieval. In *Proceedings of the IEEE/CVF International Conference on Computer Vision*, pages 13576–13586, 2023.

[82] Peijun Bao, Zihao Shao, Wenhan Yang, Boon Poh Ng, Meng Hwa Er, and Alex C Kot. Omnipotent distillation with llms for weakly-supervised natural language video localization: When divergence meets consistency. In *Proceedings of the AAAI Conference on Artificial Intelligence*, volume 38, pages 747–755, 2024.

[83] Peijun Bao, Yong Xia, Wenhan Yang, Boon Poh Ng, Meng Hwa Er, and Alex C Kot. Local-global multi-modal distillation for weakly-supervised temporal video grounding. In *Proceedings of the AAAI Conference on Artificial Intelligence*, volume 38, pages 738–746, 2024.

[84] Ze Liu, Yutong Lin, Yue Cao, Han Hu, Yixuan Wei, Zheng Zhang, Stephen Lin, and Baining Guo. Swin transformer: Hierarchical vision transformer using shifted windows. In *Proceedings of the IEEE/CVF International Conference on Computer Vision*, pages 10012–10022, 2021.

[85] Alec Radford, Jong Wook Kim, Chris Hallacy, Aditya Ramesh, Gabriel Goh, Sandhini Agarwal, Girish Sastry, Amanda Askell, Pamela Mishkin, Jack Clark, et al. Learning transferable visual models from natural language supervision. In *International Conference on Machine Learning*, pages 8748–8763. PMLR, 2021.

[86] Junnan Li, Dongxu Li, Caiming Xiong, and Steven Hoi. Blip: Bootstrapping language-image pre-training for unified vision-language understanding and generation. In *International Conference on Machine Learning*, pages 12888–12900. PMLR, 2022.

[87] OpenAI. Gpt-4 technical report. 2023.

[88] Junbin Xiao, Pan Zhou, Tat-Seng Chua, and Shuicheng Yan. Video graph transformer for video question answering. In *European Conference on Computer Vision*, pages 39–58, 2022.

[89] Ross Girshick, Jeff Donahue, Trevor Darrell, and Jitendra Malik. Rich feature hierarchies for accurate object detection and semantic segmentation. In *Proceedings of the IEEE Conference on Computer Vision and Pattern Recognition*, pages 580–587, 2014.

[90] Jacob Devlin. Bert: Pre-training of deep bidirectional transformers for language understanding. *arXiv preprint arXiv:1810.04805*, 2018.

[91] Tsu-Jui Fu, Linjie Li, Zhe Gan, Kevin Lin, William Yang Wang, Lijuan Wang, and Zicheng Liu. An empirical study of end-to-end video-language transformers with masked visual modeling. In *Proceedings of the IEEE/CVF Conference on Computer Vision and Pattern Recognition*, pages 22898–22909, 2023.

[92] Ze Liu, Jia Ning, Yue Cao, Yixuan Wei, Zheng Zhang, Stephen Lin, and Han Hu. Video swin transformer. In *Proceedings of the IEEE/CVF Conference on Computer Vision and Pattern Recognition*, pages 3202–3211, 2022.

[93] Yinhan Liu. Roberta: A robustly optimized bert pretraining approach. *arXiv preprint arXiv:1907.11692*, 364, 2019.

[94] Alexey Dosovitskiy. An image is worth 16x16 words: Transformers for image recognition at scale. *arXiv preprint arXiv:2010.11929*, 2020.

[95] Pengcheng He, Xiaodong Liu, Jianfeng Gao, and Weizhu Chen. Deberta: Decoding-enhanced bert with disentangled attention. *arXiv preprint arXiv:2006.03654*, 2020.

[96] Laurens Van der Maaten and Geoffrey Hinton. Visualizing data using t-sne. *Journal of Machine Learning Research*, 9(11), 2008.